THE JOURNAL OF BIOLOGICAL CHEMISTRY
Vol. 276, No. 33, Issue of August 17, pp. 31340–31348, 2001

Printed in U.S.A.

Interactions between Adaptor Protein-1 of the Clathrin Coat and Microtubules via Type 1a Microtubule-associated Proteins*

Received for publication, February 4, 2001, and in revised form, May 1, 2001
Published, JBC Papers in Press, June 19, 2001, DOI 10.1074/jbc.M101054200

Ena Orzech, Leonid Livshits, Julieta Leyt, Hana Okhrimenko, Vanda Reich, Shulamit Cohen, Aryeh Weiss§, Naomi Melamed-Book‡, Mario Lebendiker¶, Yoram Altschuler‖, and Benjamin Aroeti**

From the Department of Cell and Animal Biology, the ¶Protein Purification Unit, and the Wolfson Center for Applied Structural Biology, the ‡Department of Biological Chemistry, Institute of Life Sciences, Hebrew University of Jerusalem, Jerusalem 91904, Israel, the §Department of Electronics, Jerusalem College of Technology, Jerusalem 91160, Israel, and the ‖Department of Pharmacology, School of Pharmacy, Faculty of Medicine, Hebrew University of Jerusalem, Jerusalem 91120, Israel

The classical view suggests that adaptor proteins of the clathrin coat mediate the sorting of cargo protein passengers into clathrin-coated pits and the recruitment of clathrin into budding areas in the donor membrane. In the present study, we provide biochemical and morphological evidence that the adaptor protein 1 (AP-1) adaptor of the *trans*-Golgi network clathrin interacts with microtubules. AP-1 in cytosolic extracts interacted with *in vitro* assembled microtubules, and these interactions were inhibited by ATP depletion of the extracts or in the presence of 5′-adenylylimidodiphosphate. An overexpressed γ-subunit of the AP-1 complex associated with microtubules, suggesting that this subunit may mediate the interaction of AP-1 with the cytoskeleton. Purified AP-1 did not interact with purified microtubules, but interaction occurred when an isolated microtubule-associated protein fraction was added to the reaction mix. The γ-adaptin subunit of AP-1 specifically co-immunoprecipitated with a microtubule-associated protein of type 1a from rat brain cytosol. This suggests that type 1a microtubule-associated protein may mediate the association of AP-1 with microtubules in the cytoplasm. The microtubule binding activity of AP-1 was markedly inhibited in cytosol of mitotic cells. By means of its interaction with microtubule-associated proteins, we propose novel roles for AP-1 adaptors in modulating the dynamics of the cytoskeleton, the stability and shape of coated organelles, and the loading of nascent AP-1-coated vesicles onto appropriate microtubular tracks.

In eukaryotic cells, transport of proteins between membrane-bound compartments along the exocytic and endocytic pathways is mediated by coated carrier vesicles that bud from the donor compartment and fuse with a target acceptor compartment(s). The coats are commonly divided into two groups: the clathrin-based coats and the nonclathrin coatomers. Coat proteins are recruited to the cytoplasmic surface of the donor organelle membrane from a cytosolic pool, and this process is thought to be regulated by specific small GTP-binding proteins. Upon binding to an organelle, coat proteins are believed to serve two main functions: 1) to promote selective sorting of protein passengers into budding areas in the donor organelle and hence into the nascent carrier vesicle (this process is mediated by coat protein recognition of short cytoplasmic amino acid stretches, termed sorting signals) and 2) to initiate local membrane deformation (bending) required for the formation of transport vesicle from a physically stable donor membrane. Following vesicle formation, the coat material is removed, and the coat-free carrier vesicle travels along cytoskeletal tracks toward its acceptor membrane.

Considerable progress has been made during the last few years toward the understanding of the structure and function of clathrin-based coats (for recent reviews, see Refs. 1 and 2). Clathrin coats are assembled from two major components: clathrin and adaptor complexes (adaptor proteins; APs).[1] APs are recruited from the cytosol onto the cytoplasmic surface of two distinct organelles: the plasma membrane and the *trans*-Golgi network (TGN). The binding of APs is essential for the subsequent assembly of cytosolic clathrin on the donor membrane, and hence for the subsequent vesicle formation. The accepted mechanism is that the assembly of cytosolic clathrin forms the scaffold required for the local deformation of membrane and for the subsequent formation of clathrin-coated vesicles (CCVs). AP-2 complexes drive the formation of clathrin-coated endocytic vesicles from the plasma membrane, whereas AP-1 complexes prompt the formation of exocytic transport vesicles in the TGN. Ultrastructural studies suggest a low level of AP-1 association with endosomes (1). In addition, an AP-1-related complex localized neither to the TGN nor to endosomal compartments has recently been identified (3).

Both AP-1 and AP-2 complexes are heterotetramers, consisting of two large subunits termed adaptins (γ and β_1 in the case of AP-1; α and β_2 in the case of AP-2), a medium-sized subunit (μ_1 or μ_2), and a small subunit (σ_1 or σ_2). The primary function of the β-subunit is to bind clathrin, but it may also be involved in the recognition of dileucine-based sorting signals (4). The γ

* This research was supported by a grant from the Israel Science Foundation founded by the Israel Academy of Sciences and in part by a grant from the United States-Israel Binational Science Foundation (Jerusalem, Israel) Grant 1999277. The costs of publication of this article were defrayed in part by the payment of page charges. This article must therefore be hereby marked "*advertisement*" in accordance with 18 U.S.C. Section 1734 solely to indicate this fact.

** To whom correspondence should be addressed. Fax: 972-2-5617918; E-mail: aroeti@cc.huji.ac.il.

[1] The abbreviations used are: AP, adaptor protein; TGN, *trans*-Golgi network; MAP, microtubule-associated protein; MDCK, Madin-Darby canine kidney; MCT, MAP-containing tubulin; MFT, MAP-free monomeric tubulin; WB, Western blotting; IF, immunofluorescence; CCVs, clathrin-coated vesicles; Dox, doxycycline; MT, microtubule; AMP-PNP, 5′-adenylylimidodiphosphate; Pipes, 1,4-piperazinediethanesulfonic acid; MEM, minimal essential medium; BSA, bovine serum albumin; PBS, phosphate-buffered saline; PAGE, polyacrylamide gel electrophoresis; BFA, brefeldin A.

and α adaptins most likely contain targeting information in a 200-residue region within the N-terminal core domain (5). μ_{1A}, the ubiquitous chain of the AP-1 adaptor complex, may also have some function in AP-1 binding to the TGN and the recognition of tyrosine-based sorting signals encoded by cargo proteins (1). An epithelium-specific μ-chain version, μ_{1B}, has recently been cloned and implicated in basolateral targeting of specific receptors (6). The function of the σ subunit is unknown.

Although considerable progress has been made in recent years in resolving problems of recognition, specificity, and regulation of cargo/AP/clathrin interactions, we still lack a deep mechanistic understanding of how APs are involved in the formation of transport vesicles, and whether they are involved in downstream events of vesicle transport. Also, the need for APs in clathrin coat formation remains unresolved (1). Simultaneous disruption of all known AP subunits in yeast, for example, failed to generate the clathrin minus phenotype and has no noticeable effect on the generation of clathrin-coated vesicles and cell cycle in the mutant yeast (7). However, knockout experiments in which the μ_{1A}-subunit gene has been deleted in mice indicated a key function for AP-1 in endosomal sorting of mannose 6-phosphate receptors (8), and when the γ-adaptin gene was deleted in mice, mouse embryos died at a very early stage of development (9). These results suggest that AP complexes, including AP-1 adaptors, play more important roles in multicellular organisms than in yeast.

But these observations also raise general concerns related to AP functions. It is possible, for instance, that the severe failure of multicellular organization associated with γ-adaptin deletion is due to general malfunction in clathrin coat assembly. Another possibility is that AP-1 complexes perform additional, yet unrecognized, cellular functions uniquely expressed in Metazoa.

In this paper, we show that AP-1 adaptors are capable of interacting with microtubules (MTs) via scaffolding proteins belonging to the structural MT-associated protein (MAP) family. Structural MAPs promote tubulin polymerization, stabilize MTs often in the form of bundles, function as molecular spacers linking microtubular tracks, and interact with F-actin (for reviews see Refs. 10 and 11). The increasing stability of MTs is thought to be critical for neuronal morphogenesis and the development of cell polarity (12). On the basis of this knowledge and our data we propose that ubiquitous MAPs (*e.g.* microtubule-associated protein of type 1A (MAP1a)) are involved in loading AP-1-bearing transport vesicles onto appropriate MTs. AP-1-MAP interactions may also modulate the stability of MTs and the structure of AP-1-coated organelles.

EXPERIMENTAL PROCEDURES

Materials

Tubulin purified from calf brain, containing ~85% tubulin and 15% associated proteins (MAP-containing tubulin; MCT), was prepared by heat-dependent assembly-disassembly cycles (kindly provided by Dr. Pnina Yaish (Sigma). MCT was provided as a lyophilized powder containing MES buffer salts, EGTA, EDTA, $MgCl_2$, dithiothreitol, GTP, leupeptin, aprotinin, and sucrose as stabilizer. The powder was reconstituted in H_2O supplemented with 100 μM paclitaxel (Taxol) to yield 10 mg/ml protein concentration. MTs were assembled according to protocols provided by the manufacturer. Taxol was purchased from Sigma. Latrunculin A was a generous gift from Prof. Yoel Kashman (School of Chemistry, Tel-Aviv University). Methyl-(5-(2-theinyl-carbonyl)-1H-benzimidazol-2-yl)carbamate (nocodazole) was from Sigma. AMP-PNP was from Sigma. Protein A-Sepharose beads were from Pierce.

Antibodies

Affinity-purified rabbit anti-γ-adaptin was used at a 1:100 dilution for immunofluorescence. Antibodies directed against the μ_1 and σ_1 adaptor subunits were used as previously described (13). Mouse anti-γ-adaptin monoclonal antibodies, clone 100/3, were purchased from Sigma. These antibodies were used at 1:250 dilution for immunofluorescence (IF) and at 1:1000 dilution for Western blotting (WB). Mouse polyclonal antibodies directed against mouse-γ-adaptin proline/glycine-rich hinge domain were from Transduction Laboratories. In experiments in which γ-adaptin was overexpressed in Madin-Darby canine kidney (MDCK) cells, the overexpressed subunit could be exclusively labeled with these antibodies if used at a 1:100 dilution for IF, or at 1:5000 for WB. Rabbit anti-TGN38 has been used for IF as described (14). Monoclonal antibodies anti-α-tubulin (clone B-5-1-2) from Sigma were used at 1:100 and 1:1000 dilution for IF and WB, respectively. Mouse monoclonal antibodies immunospecific for MAP1a (clone HM-1), which react with the mouse and rat proteins, were from Sigma. Mouse monclonal 100/2 directed against α-adaptin was from Sigma and used at 1:100 dilution for immunoblotting. Mouse monoclonal anti-tau (15) was used at 1:1000 dilution for WB. Mouse monoclonal anti-p58 antibodies were from Sigma and used at 1:100 for IF. The rat monoclonal anti-yeast tubulin, clone YL1/2 (1:400 for IF), was obtained from Dr. M. Brandeis (Hebrew University, Israel). Purified mouse IgG1 was from Sigma. Secondary antibodies labeled with horseradish peroxidase or with fluorescent probes were from Jackson ImmunoResearch. Protease inhibitors were from Roche Molecular Biochemicals or Sigma.

Cells

MDCK cells were cultured on plastic dishes or coverslips as previously described (16). The embryonic carcinoma cell line, P19, was obtained from Dr. M. Linial (Hebrew University, Israel). Cells were cultured and differentiated as described (17).

Purification of MAP-free MTs and Isolation of the MAP Fraction

Tubulin was purified from bovine brain with four cycles of polymerization-depolymerization followed by chromatography on phosphocellulose P11 column, essentially as described by Williams (18). The purified MAP-free monomeric tubulin (MFT, ~4 mg/ml) was aliquoted, frozen in liquid nitrogen, and stored at −80 °C. MAPs were eluted from the P11 column with 1 M KCl and concentrated through Centricon to yield a protein concentration of 2 mg/ml. The concentrated MAP fraction was aliquoted, snap-frozen in liquid N_2, and stored at −80 °C.

For the *in vitro* co-sedimentation assay, an aliquot of 4 mg of monomeric tubulin was polymerized at 37 °C for 30 min in PEM (100 mM K-Pipes, pH 6.8, 0.5 mM $MgCl_2$, 1 mM EDTA) containing 1 mM dithiothreitol, 1 mM Mg-GTP, 1 mM Mg-ATP, and 20 μM Taxol. The polymerized tubulin was centrifuged twice (55,000 rpm TLS rotor, 30 min 22 °C) through a 10% sucrose cushion containing 20 μM Taxol. The pellet was gently resuspended in PEM-containing Taxol to yield a 3 mg/ml protein concentration. Aliquots were snap-frozen and stored at −80 °C.

Treatment with Nocodazole and Latrunculin A

MDCK monolayers grown on plastic plates were washed three times with MEM/BSA (MEM containing 0.25 g/liter $NaHCO_3$, 0.6% BSA, and 20 mM HEPES, pH 7.4), and actin filaments were depolymerized by incubating the cells in MEM/BSA supplemented with 5 μM latrunculin A for 60 min at 37 °C. The latrunculin A stock solution (10 mM in Me_2SO) was stored at −20 °C. MTs were depolymerized by incubating MDCK cells for 30 min at 4 °C in MEM/BSA, followed by a 60-min incubation in MEM/BSA supplemented with 33 μM nocodazole for 60 min at 4 °C and subsequent treatment for 60 min with the drug added in warm (37 °C) MEM/BSA. The nocodazole stock solution (33 mM in Me_2SO) was stored at −20 °C.

Immunofluorescence and Confocal Microscopy

Cells were fixed for 10 min in methanol at −20 °C or fixed with paraformaldehyde according to the pH shift fixation procedure (19) and processed for immunofluorescence as previously described (13). When staining with rhodamine-phalloidin, cells were fixed by the paraformaldehyde pH shift method and then stained in PBS with 5 units/ml rhodamine phalloidin (stock solution stored as 200 units/ml in methanol at −20 °C) for 30 min at 22 °C. Cells were washed three times for 5 min with PBS, postfixed, mounted, and stored as described (19). A Bio-Rad MRC-1024 confocal scanhead coupled to a Zeiss Axiovert 135M inverted microscope fitted with × 40 or × 63 oil immersion lenses was used to acquire images of the stained cells as described (13). Images (512 × 512 pixels) were saved in tag information file format, and contrast levels of each image were adjusted in the Photoshop program (Adobe, Mountain View, CA). Contrast-corrected images were imported into Freehand (Macromedia, San Francisco, CA).

Preparation of Purified AP-1 Complexes

AP-1 and AP-2 complexes were isolated from CCVs obtained from 150 bovine adrenal glands using gel filtration chromatography (65 × 1.6 cm Sephacryl S300 HR columns; Amersham Pharmacia Biotech), and AP-1 was further purified from AP-2 by hydroxyapatite (1-ml Econo-Pac HTP cartridge; Bio-Rad) chromatography. The absence of AP-2 in AP-1-containing samples was confirmed by immunoblotting, using the 100/2 antibodies. Both purification steps were performed by fast protein liquid chromatography (Amersham Pharmacia Biotech EktaExplorer), following previously established protocols (20). Samples containing purified AP-1 (1 mg/ml) were snap-frozen and stored at −80 °C.

Binding of AP-1 to MTs

The MT binding activity of cytosolic AP-1, or of AP-1 purified from CCVs, was examined by the MT cosedimentation assay.

Preparation of MDCK, Rat Liver, and Rat Brain Cytosol—For each experiment, fresh cytosol was prepared from confluent MDCK monolayers cultured for 3 days on three 10-cm plates. Cytosol extraction was performed at 4 °C using ice-cold and freshly prepared buffers. Cells were washed three times with 10 ml of PBS, pH 7.4, and once with 10 ml of PMEE buffer (PEM buffer containing 0.5 mM EGTA) supplemented with 1 mM phenylmethylsulfonyl fluoride, a mixture of protease inhibitors (25 μg/ml pepstatin, 50 μg/ml chymostatin, 25 μg/ml leupeptin, 50 μg/ml antipain, 2.5 μg/ml aprotinin), and 250 mM sucrose (PMEE/sucrose). Buffer was aspirated, leaving cell monolayers as dry as possible. 0.3 ml of PMEE/sucrose buffer was added to each plate, and cells were scraped off the dish by a rubber policeman. Cell suspensions from each plate were combined into a single Eppendorf tube, and cells were then broken by 10 passages through a 21-gauge needle followed by 10 passages through a 25-gauge needle connected to a 1-ml syringe. Homogenate was ultracentrifuged (60,000 rpm, TLA120.2 rotor; 45 min at 4 °C). The supernatant (cytosol) was separated from the membrane pellet and kept on ice. Rat liver and rat brain cytosol were prepared from 10–15 3½-month-old Sabra rats, as described (21). To prepare mitotic cytosol, a suspension of mitotic cells (see below) was spun, and cell pellet was suspended in an equal volume of PMEE/sucrose buffer.

Cytosol depleted of endogenous tubulin was prepared as follows. Cytosol was incubated for 30 min at 37 °C with 1 mM Mg-GTP and 20 μM Taxol final concentrations. Cytosol was then centrifuged (60,000 TLA120.2 rotor; 15 min at 22 °C), and supernatant (tubulin-depleted cytosol) was carefully transferred to a fresh Eppendorf tube. In some experiments, MDCK cytosol was depleted of ATP by incubation with 10 mg/ml glucose and 2 units of hexokinase (type C-130; Sigma) for 15 min at 22 °C, or cytosol was supplemented with 2 mM AMP-PNP.

MT Cosedimentation Assay—Cytosol free of endogenous tubulin (100 μg/ml final concentration) or purified AP-1 (125 μg/ml final concentration) was first centrifuged (30,000 rpm, 15 min, 22 °C, Ti-42.2 Backman rotor) to pellet protein aggregates. Cytosol was incubated with Taxol-stabilized polymeric tubulin (9 μM) assembled from either MCT or MFT for 30 min at 22 or 37 °C, as indicated under "Results." Similarly, AP-1 purified from CCVs was incubated with MAP-free polymeric tubulin, in the absence or presence of MAPs (100 μg/ml final concentration). The final volume of the reaction mixture was 40 μl. The reaction mixture was centrifuged for 30 min (20,000 rpm, Ti-42.2 Beckman rotor, 22 °C). Following centrifugation, γ-adaptin associated with polymeric tubulin was in the pellet, whereas γ-adaptin that does not interact with polymeric tubulin remains in the cytosol supernatant. The entire supernatant (unless otherwise stated) and pellet were solubilized in 2× sample buffer (1× sample buffer: 15 mM Tris-HCl, pH 6.8, 25 mM EDTA, pH 7.0, 0.25% urea mixed with bromphenol blue, 6% (v/v) glycerol, 65 mM dithiothreitol) and analyzed for the presence of γ-adaptin by SDS-PAGE followed by WB (13).

Co-immunoprecipitations

γ-Adaptin with Tubulin—Anti-α-tubulin (Sigma) or irrelevant mouse IgG1 antibodies (Sigma) were covalently coupled to protein A-Sepharose using dimethylpimelimidate as previously described (16). Freshly prepared MDCK cytosol was supplemented with 5 mM Mg-ATP and then precleared by its incubation for 4 h at 4 °C with 250 μl of plain protein A-Sepharose. After spinning down the beads, the cleared cytosol was transferred to an Eppendorf tube containing 50 μl of plain protein A-Sepharose, protein A-Sepharose coupled to IgG, or protein A-Sepharose coupled to anti-tubulin. The cytosol was incubated with the beads for 15 h at 4 °C. Beads were then washed six times with cold PEM buffer, and proteins were released by boiling the beads in SDS-PAGE sample buffer. The presence of tubulin and γ-adaptin in the immunoprecipitates was detected by immunoblotting.

γ-Adaptin with MAP1a—A 2-μl aliquot of monoclonal anti-MAP1a (clone HM1, Sigma) and of irrelevant mouse IgG1 antibodies (Sigma) were diluted into 0.5 ml of PEM buffer, incubated with protein A-Sepharose (100 μl, 15% slurry; Amersham Pharmacia Biotech) for 15–17 h at 4 °C with rotation, and subsequently covalently attached to the beads by dimethylpimelimidate. Antibody-coupled beads were washed four times with PEM buffer supplemented with 0.1% Nonidet P-40 (PEM/Nonidet P-40). Brain rat cytosol was thawed, supplemented with protease inhibitors, and spun for 15 min at 4 °C (15,000 × *g*) to eliminate large protein aggregates. The cytosol was then diluted with buffer PEM/Nonidet P-40 to yield 2 mg/ml protein concentration. Antibody-coupled beads were incubated with 0.5 ml of cytosol for 15–17 h at 4 °C with continuous end-to-end rotation. Immunobeads were then washed six times with buffer PEM/Nonidet P-40 and one time with buffer PEM, dried, mixed with 2× SDS-PAGE sample buffer, and boiled for 3 min to release the bound material. For MAP1a detection, half of the sample buffer volume was subjected to SDS-PAGE using 7% polyacrylamide gel; for γ-adaptin detection, the rest of the sample was analyzed by 10% gels. MAP1a immunoprecipitates were transferred to nitrocellulose sheets using the Bio-Rad Mini Trans-Blot® wet electrophoretic transfer cell apparatus (240 mA, 2 h). The γ-adaptin immunoprecipitates were transferred to nitrocellulose membranes using the Hoefer semidry apparatus as previously described. Nitrocellulose sheets were blocked and probed with anti-MAP1a antibody (1:500) or with anti-γ-adaptin antibodies (1:1000; Transduction Laboratories).

Mitosis Assay—Confluent MDCK monolayers cultured on 10-cm plates were split 1:10. After 16 h, cells were trypsinized, and 4×10^5 cells were seeded on a 10 cm dish. Cells were allowed to settle on the plate for an additional 6 h. Then 0.33 μM nocodazole was added to the growth medium, and cells were incubated in the presence of nocodazole for about 11 h at 37 °C in CO_2 incubator. Mitotic cells, typically arrested in prometaphase, were collected by the mitotic shake-off procedure, as described (22). For immunofluorescence, harvested mitotic cells were gently placed on top of a coverslip precoated with a 50% solution of polylysine (Sigma). Tight attachment to the coverslip was promoted by brief centrifugation.

Adenovirus-mediated Expression of γ-Adaptin—The mouse γ-adaptin cDNA was subcloned in the sense direction into the *Bam*HI sites of the pADtet vector containing the regulated tetracycline promotor. Adenoviruses were produced as described (23). MDCK cells (T23 clone, which constitutively expresses the *trans*-activator of the *tet* system) were seeded at confluence 4 days prior the assay on 12-mm Transwell™ (Costar). 18 h before the assay, cells were infected at their apical side for 2 h with 5 μl of the γ-adaptin virus stock, corresponding to ~40 plaque-forming units/cell in PBS containing 1 mM $MgCl_2$ but lacking $CaCl_2$. Cells were washed twice with PBS containing 1 mM $MgCl_2$. Expression of γ-adaptin was induced by incubating the cells for a further 16 h in MEM containing Earle's balanced salt solution supplemented with 5% fetal bovine serum, 100 units/ml penicillin, 100 mg/ml streptomycin, in 5% CO_2 and 95% air at 37 °C and humidified atmosphere. Expression was suppressed by incubating the infected cells for 16 h in medium containing 20 ng/ml doxycycline (Dox; Sigma). The Dox stock solution (1 mg/ml in H_2O, stored at −80 °C) was diluted to the indicated concentration just before use. Using this method, 95–100% of the filter-cultured T23 cells expressed the γ-adaptin, as judged by immunofluorescence analysis.

RESULTS

Analysis of γ-Adaptin-Tubulin Interactions by Confocal Microscopy and by Co-immunoprecipitation—MDCK cell monolayers were treated with nocodazole, immunostained with anti-γ-adaptin antibodies, and prepared for immunofluorescence confocal microscopy. Nocodazole treatment disrupts the typical perinuclear staining of γ-adaptin (Fig. 1*A*, compare *Nocodazole* with *Control*). The transmembrane TGN marker, TGN38, was also dispersed in the cell cytoplasm in nocodazole-treated cells (Fig. 1*A*). Note that some γ-adaptin staining remained at supranuclear regions (indicated by *arrows*), suggesting the existence of a γ-adaptin population that is resistant to nocodazole treatment. In these regions, AP-1 may interact with nocodazole-insensitive cytoskeletal elements. Following nocodazole removal, the majority of γ-adaptin and TGN38 reappeared at the perinuclear (original) location (not shown), indicating that the effects of nocodazole treatment are reversible. Cell treat-

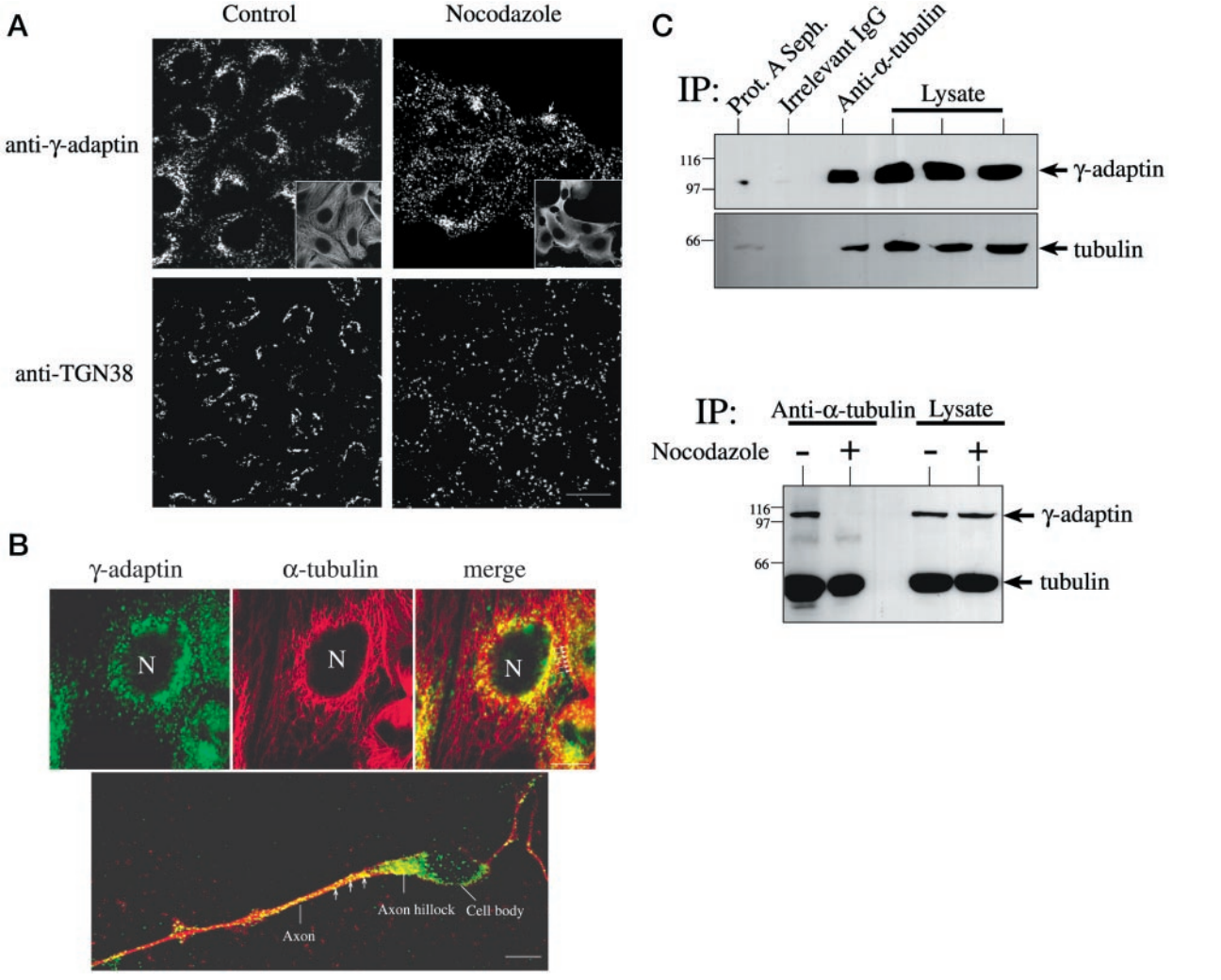

FIG. 1. **Immunofluorescence confocal microscopic and co-immunoprecipitation analyses of γ-adaptin interaction with MTs.** *A*, distribution of γ-adaptin and TGN38 following nocodazole treatment. Coverslip-grown MDCK cells were treated with nocodazole, fixed with methanol, and labeled with the anti-γ-adaptin 100/3 antibody or with rabbit polyclonal antibodies directed against TGN38. Samples were processed for analysis by confocal microscopy, and representative optical sections are shown. The *arrows* point toward juxtanuclear γ-adaptin-labeled structures not dispersed by nocodazole. Intracellular distribution of MTs in control- and nocodazole-treated cells is presented in *insets*. *Bar*, 10 μm. *B*, γ-adaptin resides in the vicinity of MTs. Coverslip cultured MDCK (*upper panel*) or neuronal P19 cells (*lower panel*) were fixed in cold methanol. MDCK cells were incubated with affinity-purified rabbit anti-γ-adaptin and mouse anti-α-tubulin monoclonal antibodies, whereas P19 cells were incubated with anti-γ-adaptin mouse antibodies (Transduction Laboratories) and with the rat monoclonal anti-tubulin YL1/2, followed by fluorescein isothiocyanate (*green*) or Texas Red (*red*)-conjugated secondary antibodies. The anti-mouse secondary antibody does not recognize rat antibodies, and *vice versa*. Confocal optical sections were taken and processed as described under "Experimental Procedures." The *arrows* indicate a row of punctate γ-adaptin-labeled structures possibly positioned along MT tracks. *N*, nucleus. *Bar*, 10 μm. *C*, γ-adaptin co-immunoprecipitates with tubulin from MDCK cytosol. Cytosol from MDCK cells, treated or not with nocodazole, was subjected to immunoprecipitation (*IP* refers to antibody used for immunoprecipitation) with anti-α-tubulin antibodies. The ability of γ-adaptin to co-immunoprecipitate with tubulin was examined as specified under "Experimental Procedures." Molecular mass markers are indicated in kDa.

ment with the actin-disrupting agent, latrunculin A, did not affect the intracellular distribution of γ-adaptin (data not shown). It is possible that Golgi disruption by nocodazole is the mere cause for γ-adaptin dispersal in nocodazole-treated cells, regardless of whether AP-1 is attached to MTs or not (24, 25). Another possibility, however, is that AP-1 links the organelle to MTs, and MT disruption by nocodazole results in a concomitant dispersion of AP-1-coated organelles.

Our next aim was to determine whether AP-1 co-localizes with microtubular arrays. To investigate this, γ-adaptin and tubulin in MDCK cells and differentiated P19 neuronal cells were fluorescently immunolabeled (in *green* and *red*, respectively), and their respective intracellular distribution was analyzed by confocal microscopy. High magnification images of single MDCK cells (Fig. 1*B*, *upper panel*) reveal two populations of γ-adaptin-labeled structures. A small fraction of γ-adaptin-labeled organelles appeared mainly as linear tracks of punctate/vesicular staining, coinciding with MTs (indicated by *arrows* in the *merge panel*). These structures may represent γ-adaptin-coated vesicles associated with MTs. The majority of γ-adaptin labeling, although seen in regional proximity with microtubular networks, did not co-localize with MTs. Interestingly, γ-adaptin-coated organelles were also seen in tubulin-rich axonal regions in P19 cells (Fig. 1*B*, *lower panel*, structures indicated by *arrows*). These morphological observations suggest that some AP-1 adaptor-coated organelles and perhaps cytosolic AP-1 exist in regional proximity with MTs.

To further assess the possible interactions between AP-1 and MTs, the ability of γ-adaptin to co-immunoprecipitate with tubulin from MDCK cytosolic extracts was investigated. Tubulin was immunoprecipitated from MDCK cytosol with monoclonal anti-α-tubulin antibodies, and the presence of γ-adaptin in the immunoprecipitates was examined by immunoblotting, as explained under "Experimental Procedures." The results

revealed that γ-adaptin efficiently co-immunoprecipitates with anti-tubulin antibodies (Fig. 1*C*, *upper panel*), whereas only a minimal level of the protein was detected following the application of plain protein A-Sepharose or protein A-Sepharose coupled to irrelevant mouse IgG. Interestingly, γ-adaptin was not co-immunoprecipitated with tubulin in cytosol extracted from nocodazole-treated cells (Fig. 1*C*, *lower panel*). These results suggest that cytosolic AP-1 adaptor interacts with tubulin assemblies in the cytosol (for further discussion, see below).

Cytosolic AP-1 Interacts with MTs in Vitro in an ATP-dependent Fashion—Next, we examined whether cytosolic AP-1 interacts with MTs *in vitro*. Taxol-stabilized MTs assembled from MCT were incubated at 22 °C with tubulin-depleted MDCK cytosol at 22 °C. The reaction mix was layered on top of a 25% sucrose cushion and centrifuged at high speed. Following centrifugation, large protein complexes (*e.g.* MTs and associated proteins) are pelleted (P), whereas small protein complexes (*e.g.* dimeric tubulin) remain in the upper phase supernatant (S). The upper layer and the pellet were subjected to WB analysis, in which the level of γ-adaptin and α-tubulin was determined quantitatively (Fig. 2*A*).

In the absence of MTs, the γ-adaptin signal was confined to the S fraction. Here we should point out that MTs assembled from MCT contain a small amount of γ-adaptin (not shown). However, its signal was not visible under the experimental conditions employed and therefore does not contribute to the signal provided by cytosolic γ-adaptin. The addition of MTs caused the majority (90%) of γ-adaptin to co-sediment with the cytoskeletal protein in the pellet. ATP depletion of cytosol by hexokinase and glucose treatment inhibited γ-adaptin association with MTs, and binding was restored when ATP was added back to the depleted cytosol. The nonhydrolyzable analog of ATP, AMP-PNP, also inhibited γ-adaptin binding when added to the cytosol. Together, these data suggest that ATP is required for AP-1 binding to MTs. In addition, it can be concluded that the endogenous ATP level in extracted cytosol is sufficient to mediate AP-1 interactions with MTs.

We next asked whether AP-1 binding to MTs can be mediated by cytosol extracted from a different source. Rat liver cytosol was incubated with MTs as above, except that in these experiments the reaction was performed at 37 °C and in the presence of MAP-free MTs (prepared from MFT). Results of three independent experiments clearly show that ~50% of the γ-adaptin in the rat liver cytosol associated with MTs and that these interactions were completely abolished by AMP-PNP (representative data are shown in (Fig. 2*B*). Similar data were obtained with rat brain cytosol (not shown). The various treatments (in Fig. 2, *A* and *B*) did not alter the distribution of α-tubulin in the S and P fractions (20 and 80%, respectively; see *inset* in Fig. 2*B*). These data suggest that cytosolic AP-1 binds to MTs *in vitro* and that ATP is required in this process. However, the results do not answer the question of whether these interactions are direct or indirect. This issue is addressed below.

Acutely Overexpressed γ-Adaptin Interacts with MTs—We raised the possibility that γ-adaptin mediates the interactions of AP-1 with MTs. This hypothesis is supported by recent affinity chromatography experiments demonstrating that the γ-adaptin ear domain interacts with MAP1a (26). To examine this hypothesis, recombinant adenoviruses encoding the mouse γ-adaptin cDNA under a tetracycline-regulated promotor were produced and used to infect the T23 clone of MDCK cells. Western blot analysis of cell lysates using polyclonal mouse anti-γ adaptin hinge domain (Transduction Laboratories) showed that expression of γ-adaptin was suppressed by supplementing the growth medium with Dox (+*Dox*) and permitted by incubating the cells in growth medium lacking Dox (−*Dox*) (Fig. 3*A*). Note that the antibodies used (anti-γ-adaptin from Transduction Laboratories) recognized the mouse and canine proteins. However, under the experimental conditions employed, and due to the high expression level, the overproduced protein was visualized exclusively (Fig. 3*A*; compare −*Dox* with *T23*).

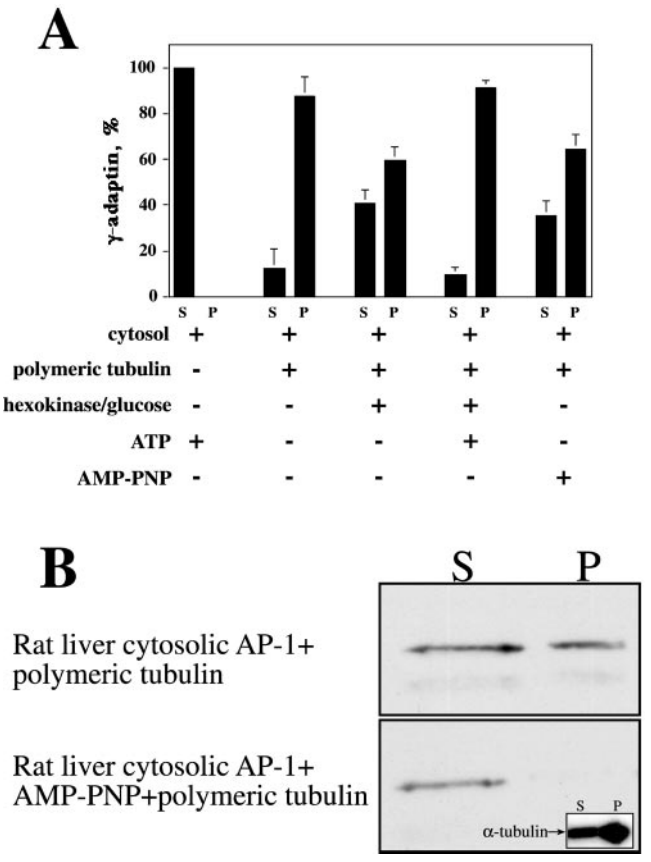

FIG. 2. ***In vitro* binding of cytosolic AP-1 to MTs.** Cytosol extracted from MDCK cells (*A*) or from rat liver (*B*) was incubated at 37 °C with polymeric tubulin assembled from MCT or MFT, respectively. The mixture was ultracentrifuged, and the pellet (*P*, polymeric tubulin) and one-fifth of the supernatant volume in the case of MDCK cytosol or the entire supernatant in the case of rat liver cytosol (*S*, monomeric tubulin), were subjected to analysis by quantitative WB. Nitrocellulose membranes were probed with anti-γ-adaptin or with anti-α-tubulin (*B*, *inset*). In all experiments, polymeric tubulin constituted ~70% of the total tubulin. In some experiments, ATP was depleted by incubating the cytosol with hexokinase and glucose; in other experiments, cytosol was supplemented with either 10 mM ATP or 2 mM AMP-PNP. Results in *A* represent the mean ± S.E. of at least five experiments. The differences between supernatant and pellet values of ATP-depleted/AMP-PNP-treated cytosol and the corresponding supernatant and pellet values of untreated cells were statistically significant ($p < 0.005$), as determined by Student's *t* test analysis. The results of three independent experiments involving rat liver cytosol were identical; representative data are depicted in *B*.

In steady state, the majority of endogenous γ-adaptin is present in complex with the μ, σ, and β′ subunits. Overexpression of γ-adaptin did not alter the expression level of σ and μ (Fig. 3*A*). At least part of the ectopic γ-adaptin is probably incorporated into the AP-1 adaptor complex, because the majority of both σ and μ subunits could be co-immunoprecipitated with the expressed protein.[2] The fact that the level of σ and μ did not change suggests that there is a pool of unassembled γ-adaptin in the overexpressing cells. Immunofluorescence analysis of the intracellular distribution of the expressed pro-

[2] E. Orzech and B. Aroeti, unpublished data.

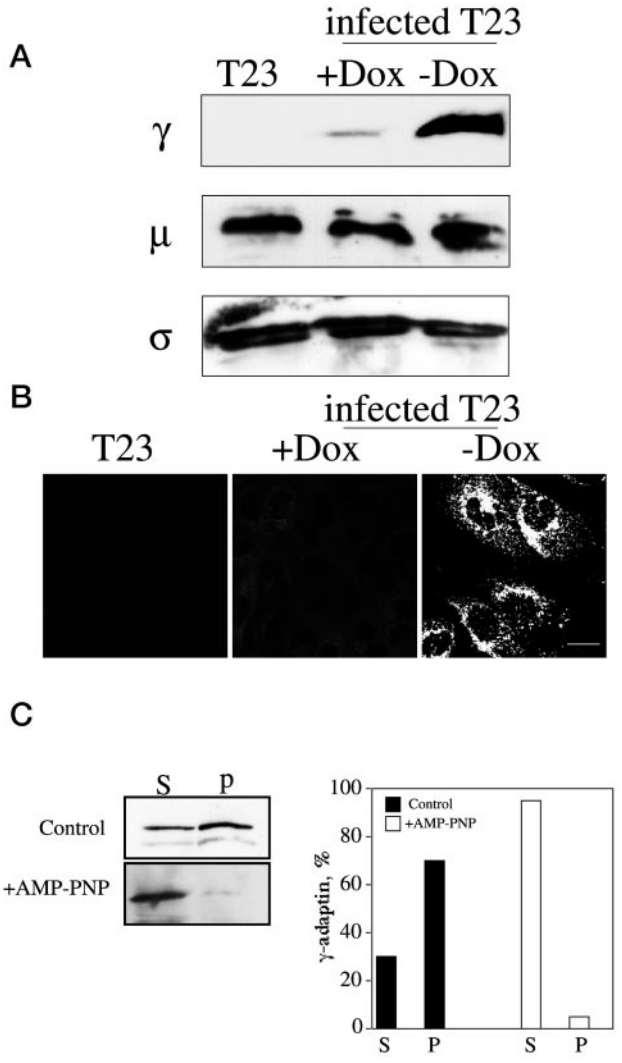

FIG. 3. **Induced overexpression of γ-adaptin in MDCK cells.** The T23 MDCK cell line was infected with recombinant adenovirus encoding the mouse γ-adaptin cDNA under the regulation of the *tet* promotor. Expression of γ-adaptin was induced by incubating the infected cells in medium lacking Dox (*−Dox*), and expression was suppressed by incubating the cells in medium containing Dox (*+Dox*). Equal protein levels of cell lysates prepared from noninfected T23 cells (T23) or from infected T23 cells were analyzed for the expression of γ-adaptin (γ) and μ- and σ-subunits by WB (*A*). The expression of γ-adaptin was also analyzed by immunofluorescence confocal microscopy (*B*). In both cases, the anti-γ-adaptin hinge domain (Transduction Laboratories) was used to detect the coat subunit. Under these conditions, the antibodies recognized exclusively the overexpressed and not the endogenous (canine) protein. *Bar*, 5 μm. The MT binding activity of overexpressed γ-adaptin was determined in the absence (*Control*, which contains only endogenous ATP) or presence of AMP-PNP (*+AMP-PNP*) using the MT co-sedimentation assay (*C*). Similar MT binding activity was observed in three independent experiments. *P*, pellet; *S*, supernatant.

tein revealed typical perinuclear localization (Fig. 3*B*, *−Dox*), consistent with expression data in another cell system (5). These results suggest that a significant fraction of overexpressed γ-adaptin is correctly targeted to perinuclear sites.

Cytosol prepared from γ-adaptin-overexpressing cells was reacted with purified MTs (assembled from MFT) at 37 °C, and the ability of the expressed protein to bind MTs was assessed by the cosedimentation assay. Data from three independent experiments demonstrate that γ-adaptin co-sediments with MTs (representative result and quantitative analysis are shown in Fig. 3*C*), suggesting that a fraction of the expressed protein interacts with MTs. As previously shown with the

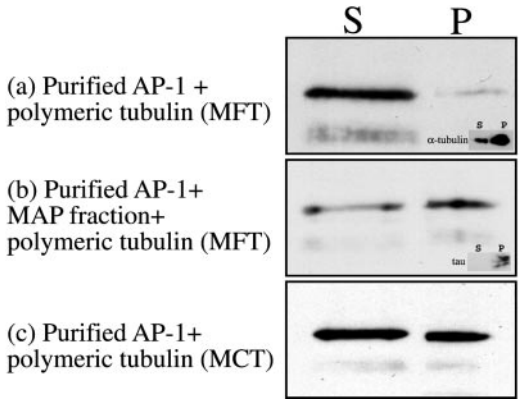

FIG. 4. **MAPs mediate AP-1 interactions with MTs.** AP-1 adaptor purified from bovine brain CCVs was incubated in PEM buffer at 37 °C with polymeric tubulin assembled from either MFT or from MCT. Samples were centrifuged, and the entire supernatant (*S*) and pellet (*P*) were analyzed for the presence of γ-adaptin by WB. Similar results were obtained in four independent experiments. Nitrocellulose sheets were also probed with anti-α-tubulin and with anti-tau (*insets*). In all cases, ~70% of tubulin was in the polymeric form, and nearly 90% of the classical MAP, tau, was found in the pellet.

native AP-1 complex (Fig. 2*A*), the addition of AMP-PNP inhibits this interaction. We conclude that γ-adaptin of the AP-1 complex mediates the interaction of AP-1 with MTs.

MAPs Are Required for AP-1 Interactions with MTs—Our next aim was to determine whether the interaction of AP-1 with MTs is direct or not. We set up an *in vitro* MT cosedimentation binding assay, in which the binding of purified AP-1 to a MAP-free MT preparation was examined. MTs were incubated with AP-1 at 37 °C, and the mixture was centrifuged to yield pellet and supernatant fractions as before. The presence of tubulin and γ-adaptin in each fraction was determined by WB. Results in Fig. 4*a* demonstrate that purified AP-1 does not interact with MAP-free MTs. However, binding was observed only when an isolated fraction of brain structural MAPs was added to the reaction mix (*b*) or when AP-1 was exposed to MTs assembled from MCT (*c*). These data suggest that AP-1 binding to MTs is indirect and that structural MAPs link the coat protein to MTs.

γ-Adaptin and Tubulin Co-immunoprecipitate with MAP1a—MAP1a is distributed in neuronal and nonneuronal tissues (27, 28). Our observation that cytosol from different sources (MDCK, rat liver, or rat brain), combined with data suggesting that MAPs isolated from brain MTs are essential for AP-1 association with MTs *in vitro*, suggested to us that a widely expressed MAP(s) interacts with AP-1. This prompted us to examine the possible association of AP-1 with MAP1a in cytosolic extracts. MAP1a was immunoprecipitated from rat brain cytosol, and the ability of γ-adaptin to co-immunoprecipitate with anti-MAP1a was examined by immunoblotting. Plain protein A-Sepharose, coupled or not to irrelevant IgG, served as negative controls. Data in Fig. 5 show that MAP1a was immunoprecipitated (the ~277-kDa heavy chain band is detected) from rat brain cytosol by the HM-1 antibodies but not by the plain protein A-Sepharose beads or by beads coupled to IgG1. Clearly, γ-adaptin and tubulin efficiently co-immunoprecipitated with anti-MAP1a. Minimal levels of these proteins were associated with the control beads, suggesting that MAP1a interacts with AP-1 and polymeric tubulin in the cytosol.

γ-Adaptin in Mitotic Cytosol Does Not Interact with MTs—We have postulated that AP-1-MAP interactions can modulate the stability of organelle and cell architecture. If so, weakening these interactions may prompt changes in organelle and cell morphology, as perhaps best exemplified during mitosis. The onset of mitosis is characterized by rapid depolymer-

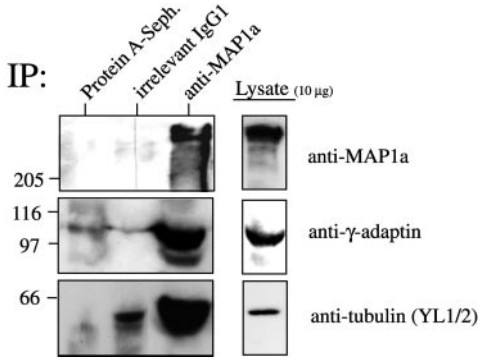

FIG. 5. **γ-Adaptin co-immunoprecipitates with anti-MAP1a.** Rat brain cytosolic extracts were exposed to plain protein A-Sepharose beads, protein A-Sepharose coupled to mouse IgG1, or protein A-Sepharose coupled to anti-MAP1a. Immunoprecipitates were analyzed by SDS-PAGE followed by WB as described under "Experimental Procedures." Nitrocellulose membranes were probed with anti-MAP1a, anti-γ-adaptin, and anti-tubulin. A representative result is presented, but similar results were obtained in two additional experiments. Molecular mass markers are indicated in kDa.

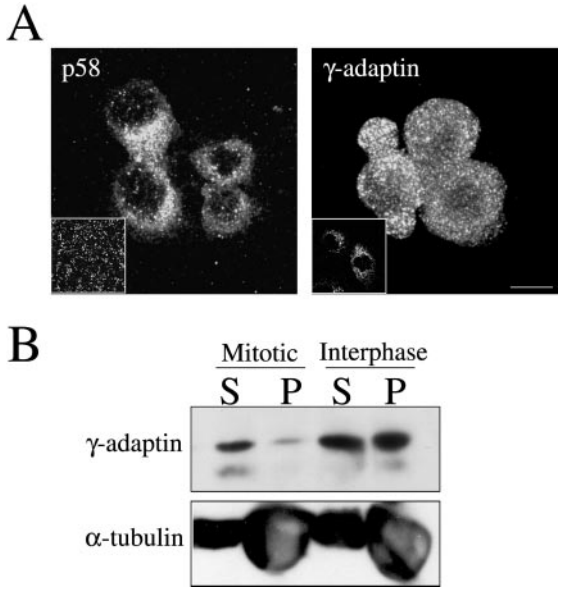

FIG. 6. **Mitotic AP-1 inefficiently associates with MTs.** MDCK cells arrested in prometaphase were harvested by the mitotic shake-off procedure. Confocal analysis of the intracellular distribution of p58 and γ-adaptin in mitotic cells and in interphase cells (*insets*) is shown in *A* (*bar*, 5 μm). Cytosol extracted from mitotic and interphase cells was subjected to the MT co-sedimentation assay, and the distribution of γ-adaptin or α-tubulin in the supernatant (*S*) and pellet (*P*) fractions was assessed by WB (*B*). Three independent experiments yielded similar results.

ization of interphase MTs and the concomitant dispersion of the Golgi apparatus throughout the cell during prophase, while during telophase, interphase MTs repolymerize, and the Golgi apparatus returns to its characteristic pericentriolar site. To confirm that the Golgi and the TGN undergo the expected morphological changes, MDCK cells were synchronized in prometaphase (by exposure to low concentration of nocodazole, as indicated under "Experimental Procedures"). Mitotic cells were then harvested and fixed, and the distribution of the Golgi peripheral protein p58 (29, 30) or the TGN γ-adaptin was followed by immunofluorescence confocal microscopy. As expected, the labeling of both proteins was associated with punctate structures distributed throughout the entire cytoplasm (Fig. 6*A*), a fluorescence pattern characteristic of disrupted organelles. Nocodazole wash-out followed by cell incubation in normal growth medium for 18 h resulted in a typical perinuclear distribution of these proteins, as in interphase cells (Fig. 6*A*, *insets*).

Cytosol prepared from mitotic MDCK cells was reacted with purified MTs, and the level of AP-1 binding was examined by the MT co-sedimentation assay. Fig. 6*B* illustrates that γ-adaptin in mitotic cytosol did not interact with the assembled MTs. In contrast, AP-1 in interphase cytosol showed typical MT binding activity. The MT binding of AP-1 in cytosol extracted from nocodazole-treated cells that remained attached to the culture dish after the harvest of mitotic cells (*i.e.* nondividing cells) was similar to MT binding of AP-1 in interphase cytosol (not shown). This confirms that the diminished MT binding activity of mitotic AP-1 was not due to the possible presence of nocodazole in the cytosolic extract.

DISCUSSION

In this study, we showed that both cytosolic AP-1 and AP-1 purified from CCVs are capable of interacting with MTs *in vitro*. Structural MAPs were essential for this binding to occur. It is reasonable to assume that MAP (structural and motors) expressed in various tissues mediated these interactions, because AP-1 adaptors in rat liver and MDCK cytosol were capable of binding to MTs. The observation that MAP1a interacts with γ-adaptin ear domain *in vitro* (26) further suggests that this specific MAP form might mediate the binding of AP-1 to MTs. To test this hypothesis, we examined whether γ-adaptin is co-immunoprecipitated with MAP1a from rat brain cytosol. Data presented in Fig. 5 suggest that is indeed the case. Interestingly, tubulin is also efficiently co-immunoprecipitated with anti-MAP1a. Since MAPs bind to polymeric tubulin, this result suggests that the cytosol contains MTs. Cytosol is, in fact, a high speed supernatant of cell extracts produced in the cold, and as such, it should consist primarily of disassembled, rather than assembled, tubulin. Interestingly, however, several reports have suggested that miniature oligomeric disassembly products of tubulin in the form of rings are formed upon cold depolymerization of MTs (31, 32). These assemblies can interact with MAPs, probably present in rat brain cytosol and possibly pulled down with the MAP1a immunoprecipitates. AP-1 may associate with these MT rings by binding to MAP1a. Similar interactions may occur with MTs in the cytoplasm of live cells.

Only a fraction (~50%) of either purified or cytosolic AP-1 typically interacted with MTs, reflecting the possible existence of multiple AP-1 populations with low or high MAP binding affinities. This notion is consistent with recent findings suggesting that AP-1 can harbor more than one type of medium (μ) chain (6, 33). ATP is required in the binding process, since ATP-depleted cytosol inhibited the binding of AP-1 to MTs (Fig. 2). The reason for this ATP dependence is not clear yet. But it is possible that protein phosphorylation (*e.g.* of AP-1 subunits (34), MAPs (12), or other interacting proteins), ATP-binding proteins, and energy-requiring processes are involved in the binding process. In this context, it is worth mentioning that a number of kinases have been identified as associated with MAP1a (35), indicating a role for these enzymes in the regulation of MAP1a functions. It is also currently not clear how AMP-PNP inhibits the binding of cytosolic AP-1 to MTs (Figs. 2 and 3). We suggest that some MT-binding proteins whose affinity to MTs increases upon binding AMP-PNP (*e.g.* the motor protein kinesin), inhibits AP-1-MAP binding to MTs, possibly by competing with MAPs on shared binding sites. Finally, it cannot be currently excluded that γ-adaptin itself is an ATP-binding protein. These assumptions, of course, have to be confirmed experimentally.

At least three potential functions can be envisaged for the

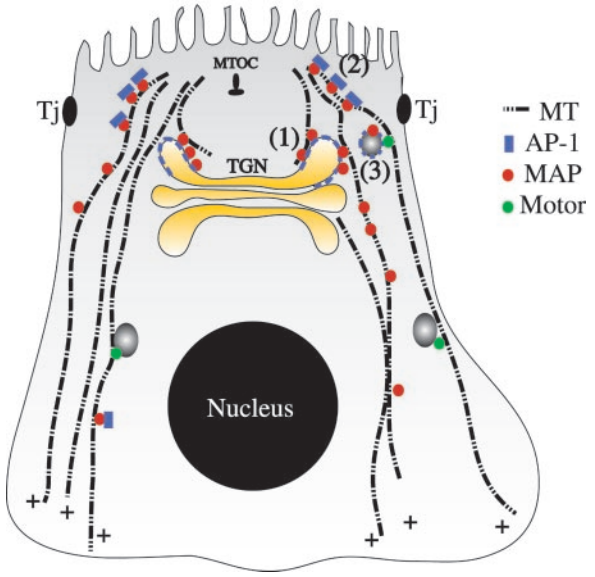

FIG. 7. **A hypothetical model for the role of AP-1-MAP-MT interactions.** A polarized epithelial cell with tight junctions (*Tj*) and intracellular organelles (*e.g.* the TGN, nucleus, and transport vesicles) are depicted. The apically positioned MT organizing center (*MTOC*) and basal plus-end MTs are indicated. AP-1-MAP-MT interactions are postulated to take place in the TGN (*1*), in the cytoplasm (*2*), and after clathrin uncoating of CCVs. The model is further discussed under "Discussion."

biological function of AP-1 association with MAPs and MTs (summarized in Fig. 7). One role could be to modulate organelle structure by anchoring the organelle's membrane to stable MTs. Golgi membranes are highly dynamic structures that undergo rapid and dramatic disassembly and reassembly (*e.g.* during mitosis and in response to drugs such as the fungal metabolite brefeldin A (BFA)). BFA treatment prevents the activation of the small GTP-binding protein, ADP-ribosylation factor type 1, resulting in the inhibition of ADP-ribosylation factor type 1-dependent coat assembly (including COP I and AP-1) on the Golgi apparatus and the TGN, respectively. The action of BFA perturbs the structure of endosomes, lysosomes, the Golgi complex, and the TGN (36, 37). BFA also induces the formation of Golgi tubules and their merging with the ER (38), as well as tubulation and merging of the TGN with endosomes (37, 39, 40). It is possible that AP-1·MAP complexes stabilize the structure of the TGN by linking the organelle's membrane to stable MTs (Fig. 7 (*1*)). Disturbance of these interactions (*e.g.* by BFA-induced inhibition of AP-1 binding to the TGN membrane) may break the link between the TGN and cytoskeleton, resulting in changes in organelle architecture (tubulation). ATP-depleted cytosol causes tubulation of Golgi membranes in the absence of BFA, *in vivo* and *in vitro* (41). Our observation that ATP depletion of cytosol inhibits the interactions between AP-1 and MTs (Fig. 3) provides a reasonable explanation of these findings. At normal ATP levels, the TGN membrane structure is stabilized by interacting with AP-1-MAP-MT scaffolds. At low ATP levels, AP-1-MT interactions could be depressed, prompting alterations in TGN structure and tubulation.

The formation of BFA-induced Golgi tubules has been shown to be driven by a cell cycle-regulated MT motor activity (42, 43). *In vitro* studies have suggested that MAPs prevent the interaction of kinesin with MTs because they form a "lawn" acting as a spacer repelling MAP-free MTs or cross-linking the MAP-containing ones (44). Dissociation of AP-1·MAP complexes from MTs may facilitate the interactions of MT motors with the organelle and promote the membrane flexibility needed for membrane tubulation and transport vesicle formation. This process may be facilitated by small GTPases belonging to the Rab and ADP-ribosylation factor families, proposed to link the TGN with kinesin-like proteins (45, 46).

A widely accepted idea suggests that ADP-ribosylation factor controls the architecture and dynamics of the Golgi by mechanisms that remain incompletely understood. ADP-ribosylation factor type 1 can stimulate spectrin binding to Golgi membranes, independent of its ability to stimulate phospholipase D or to recruit coat proteins (47). Interestingly, the γ-adaptin ear domain has also been shown to interact with β-spectrin (48). This suggests a mechanism by which assembly of spectrin immediately after ADP-ribosylation factor recruitment might generate a specialized microenvironment that allows the subsequent recruitment of AP-1. Proper and simultaneous conductance of multiple layers of interactions between AP-1, spectrin, MTs, and perhaps other cytoskeletal elements could be essential to modulate complex processes that eventually determine the structural properties of the TGN.

We still do not know if membrane-bound AP-1 associates with MAPs/MTs and whether these interactions are inhibited during mitosis. Nor do we provide any direct evidence indicating that inhibition of AP-1 binding to MTs leads to the altered organelle morphology. During the early phases of mitosis, Golgi fragmentation involves the activity of mitogen-activated protein kinase kinase (MEK1) (49) and Cdc2 (50). An intriguing hypothesis is that similar mechanisms inactivate the ability of mitotic γ-adaptin-MAP complexes to interact with MTs.

A second possible function of AP-1-MAP-MT interactions in the cytoplasm (Fig. 7 (*2*)) is that they play a role in cell morphogenesis. This hypothesis is in line with previous studies reporting that BFA treatment affects the shape and migratory properties of fibroblasts (51) as well as the shape and cytoskeletal organization of MDCK cells (52). Another example of a structural role is provided by genetic experiments, suggesting that γ-adaptin is required for apical extension growth in the fungus *Ustilago maydis* (53). These interactions may be uniquely evolved in Metazoa, because yeast cells do not express mammalian homologues of structural MAPs. This may explain why embryogenesis ceases at a very early stage of development in γ-adaptin-null transgenic mice (9), while γ-adaptin gene inactivation in yeast has no impact on cell shape or growth (7).

The third function for AP-1-MT interactions might relate to CCV post-budding events (Fig. 7 (*3*)). CCVs themselves probably cannot bind directly to MTs (54), perhaps because the clathrin lattice in CCVs masks AP-1 from binding to cytosolic components, such as MTs. The clathrin coat is rapidly released upon budding, and AP-1 is then exposed on the cytoplasmic face of the vesicle. Clathrin uncoating is promoted by the heat-shock protein, Hsc70. However, previous morphological studies have shown that while Hsc70 rapidly releases clathrin, it does not affect the APs (55, 56), and additional cytosolic factors are required to release the APs (57). These observations suggest that after clathrin removal, exposed and long lived vesicle-associated AP-1 may be functional. We suggest that it links the nascent transport vesicle to a stable microtubular track through interacting with MAPs, generating appropriate conditions for the subsequent binding of MT motors and the initiation of vesicle trafficking. Indeed, certain motor members preferentially bind to Glu (stable) tubulin-vimentin filaments (58). Also, recent data suggest that the β′ subunit of AP-1 interacts with the novel microtubule motor, KIF13A (59). Thus, it is possible that via direct interactions with microtubule-associated proteins, AP-1 regulates not only the loading but also the transport of vesicles.

In summary, we describe here a previously unknown prop-

erty of the AP-1 adaptor, the ability to interact with MTs through binding to MAPs. This feature could be essential to promote vesicle traffic, a natural extension of the classical function of AP-1 in cargo selection and coat assembly. This novel role of AP-1 is significant also because it may represent a novel molecular mechanism that couples the coat machinery with cytoskeleton-dependent processes involved in proper loading of nascent transport vesicles on the correct cytoskeleton and perhaps in cell and organelle morphogenesis.

Acknowledgments—We thank Dr. M. S. Robinson (University of Cambridge) for generous gift of affinity-purified rabbit anti-γ-adaptin, anti-μ, and anti-σ antibodies. Antibody 44 directed against TGN38 was a kind gift of Dr. G. Banting (University of Bristol). We also thank Prof. George Bloom (University of Virginia) and Prof. Irith Ginzburg (Weizmann Institute) for helpful discussions and suggestions and Dr. Allan Bar-Sinai and Prof. Marshall Devor (Hebrew University of Jerusalem) for critical reading of the manuscript.

REFERENCES

1. Kirchhausen, T. (1999) *Annu. Rev. Cell Dev. Biol.* **15,** 705–732
2. Kirchhausen, T. (2000) *Annu. Rev. Biochem.* **69,** 699–727
3. Takatsu, H., Sakurai, M., Shin, H. W., Murakami, K., and Nakayama, K. (1998) *J. Biol. Chem.* **273,** 24693–24700
4. Rapoport, I., Chen, Y. C., Cupers, P., Shoelson, S. E., and Kirchhausen, T. (1998) *EMBO J.* **17,** 2148–2155
5. Page, L. J., and Robinson, M. (1995) *J. Cell Biol.* **131,** 619–630
6. Folsch, H., Ohno, H., Bonifacino, J. S., and Mellman, I. (1999) *Cell* **99,** 189–198
7. Huang, K. M., D'Hondt, K., Riezman, H., and Lemmon, S. K. (1999) *EMBO J.* **18,** 3897–3908
8. Meyer, C., Zizioli, D., Lausmann, S., Eskelinen, E. L., Hamann, J., Saftig, P., von Figura, K., and Schu, P. (2000) *EMBO J.* **19,** 2193–2203
9. Zizioli, D., Meyer, C., Guhde, G., Saftig, P., von Figura, K., and Schu, P. (1999) *J. Biol. Chem.* **274,** 5385–5390
10. Mandelkow, E., and Mandelkow, E. M. (1995) *Curr. Opin. Cell Biol.* **7,** 72–81
11. Maccioni, R. B., and Cambiazo, V. (1995) *Physiol. Rev.* **75,** 835–854
12. Drewes, G., Ebneth, A., and Mandelkow, E. M. (1998) *Trends Biochem. Sci.* **23,** 307–311
13. Orzech, E., Schlessinger, K., Weiss, A., Okamoto, C. T., and Aroeti, B. (1998) *J. Biol. Chem.* **274,** 2201–2215
14. Orzech, E., Cohen, S., Weiss, A., and Aroeti, B. (2000) *J. Biol. Chem.* **275,** 15207–15219
15. Binder, L. I., Frankfurter, A., and Rebhun, L. I. (1985) *J. Cell Biol.* **101,** 1371–1378
16. Aroeti, B., Kosen, P. A., Kuntz, I. D., Cohen, F. E., and Mostov, K. E. (1993) *J. Cell Biol.* **123,** 1149–1160
17. Parnas, D., and Linial, M. (1995) *Int. J. Dev. Neurosci.* **13,** 767–781
18. Williams, R. C. (1992) in *The Cytoskeleton: A Practical Approach* (Carraway, K. L. and Carraway, C. A. C., eds) pp. 151–166, IRL Press, Oxford
19. Apodaca, G., Katz, L. A., and Mostov, K. E. (1994) *J. Cell Biol.* **125,** 67–86
20. Manfredi, J. J., and Bazari, W. L. (1987) *J. Biol. Chem.* **262,** 1218–12188
21. Apodaca, G., Cardone, M. H., Whiteheart, S. W., DasGupta, B. R., and Mostov, K. E. (1996) *EMBO J.* **15,** 1471–1481
22. Brandeis, M., and Hunt, T. (1996) *EMBO J.* **15,** 5280–5289
23. Hardy, S., Kitamura, M., Harris-Stansil, T., Dai, Y., and Phipps, M. L. (1997) *J. Virol.* **71,** 1842–1849
24. Holleran, E. A., and Holzbaur, E. L. (1998) *Trends Cell Biol.* **8,** 26–29
25. Lane, J., and Allan, V. (1998) *Biochim. Biophys. Acta* **1376,** 27–55
26. Hirst, J., Lui, W. W. Y., Bright, N. A., Totty, N., Seaman, M. N. J., and Robinson, M. S. (2000) *J. Cell Biol.* **149,** 67–79
27. Bloom, G. S., Luca, F. C., and Valee, R. B. (1984) *J. Cell Biol.* **98,** 331–340
28. Bloom, G. S. (1999) in *Guidebook to Cytoskeletal and Motor Proteins*, 2nd Ed. (Kreis, T. E., and Vals, R. D., eds) pp. 206–207, Oxford University Press, New York
29. Bashour, A. M., and Bloom, G. S. (1998) *J. Biol. Chem.* **273,** 19612–19617
30. Bloom, G. S., and Brashear, T. A. (1989) *J. Biol. Chem.* **264,** 16083–16092
31. Mandelkow, E. M., Mandelkow, E., and Milligan, R. A. (1991) *J. Cell Biol.* **114,** 977–991
32. Melki, R., Carlier, M. F., Pantaloni, D., and Timasheff, S. N. (1989) *Biochemistry* **28,** 9143–9152
33. Ohno, H., Tomemori, T., Nakatsu, F., Okazaki, Y., Aguilar, R. C., Foelsch, H., Mellman, I., Saito, T., Shirasawa, T., and Bonifacino, J. S. (1999) *FEBS Lett.* **449,** 215–220
34. Wilde, A., and Brodsky, M. (1996) *J. Cell Biol.* **135,** 635–645
35. Fujii, T., Watanabe, M., and Nakamura, A. (1996) *Neurochem. Int.* **28,** 535–544
36. Wagner, M., Rajasekaran, A. K., Hanzel, D. K., Mayor, S., and Rodriguez-Boulan, E. (1994) *J. Cell Sci.* **107,** 933–943
37. Lippincott-Schwartz, J., Yuan, L., Tipper, C., Amherdt, M., Orci, L., and Klausner, R. D. (1991) *Cell* **67,** 601–616
38. Lippincott-Schwartz, J., Yuan, L. C., Bonifacino, J. S., and Klausner, R. D. (1989) *Cell* **56,** 801–813
39. Wood, S. A., Park, J. E., and Brown, W. J. (1991) *Cell* **67,** 591–600
40. Reaves, B., and Banting, G. (1992) *J. Cell Biol.* **116,** 85–94
41. Cluett, E. B., Wood, S. A., Banta, M., and Brown, W. J. (1993) *J. Cell Biol.* **120,** 15–24
42. Lippincott-Schwartz, J., Cole, N. B., Marotta, A., Conrad, P. A., and Bloom, G. S. (1995) *J. Cell Biol.* **128,** 293–306
43. Robertson, A. M., and Allan, V. J. (2000) *Mol. Biol. Cell* **11,** 941–55
44. von Massow, A., Mandelkow, E.-M., and Mandelkow, E. (1989) *Cell Motil. Cytoskel.* **14,** 562–571
45. Boman, A. L., Kuai, J., Zhu, X., Chen, J., Kuriyama, R., and Kahn, R. A. (1999) *Cell Motil. Cytoskel.* **44,** 119–132
46. Echard, A., Jollivet, F., Martinez, O., Lacapere, J. J., Rousselet, A., Janoueix-Lerosey, I., and Goud, B. (1998) *Science* **279,** 580–585
47. Godi, A., Santone, I., Pertile, P., Marra, P., Di Tullio, G., Luini, A., Corda, D., and De Matteis, M. A. (1999) *Biochem. Soc. Trans.* **27,** 638–642
48. Page, L. J., Sowerby, P. J., Lui, W. W., and Robinson, M. S. (1999) *J. Cell Biol.* **146,** 993–1004
49. Lowe, M., Nakamura, N., and Warren, G. (1998) *Trends Cell Biol.* **8,** 40–44
50. Lowe, M., Gonatas, N. K., and Warren, G. (2000) *J. Cell Biol.* **149,** 341–56
51. Bershadsky, A. D., and Futerman, A. H. (1994) *Proc. Natl. Acad. Sci. U. S. A.* **91,** 5686–5689
52. Prigozina, N. L., Dugina, V. B., and Vasiliev, J. M. (1996) *Cell Biol. Int.* **20,** 379–384
53. Keon, J. P. R., Jewitt, S., and Hargreaves, J. A. (1995) *Gene* (*Amst.*) **162,** 141–145
54. Bohm, K. J., Vater, W., Steinmetzer, P., and Unger, E. (1991) *Acta Histochem. Suppl.* **41,** 65–72
55. Braell, W. A., Schlossman, D. M., Schmid, S. L., and Rothman, J. E. (1984) *J. Cell Biol.* **99,** 734–741
56. Heuser, J. E., and Keen, J. H. (1988) *J. Cell Biol.* **107,** 877–886
57. Hannan, L. A., Newmyer, S. L., and Schmid, S. L. (1998) *Mol. Biol. Cell* **9,** 2217–2229
58. Liao, G., and Gundersen, G. G. (1998) *J. Biol. Chem.* **273,** 9797–9803